

## Pion and nucleon thermal widths in the linear sigma model

C.A. Dominguez

*Institute of Theoretical Physics and Astrophysics, University of Cape Town, Rondebosch 7700, South Africa*

M. Loewe and J.C. Rojas

*Facultad de Fisica, Pontificia Universidad Catolica de Chile, Casilla 306, Santiago, Chile*

Received 1 November 1993

Editor: R. Gatto

We calculate the hadronic width (damping rate) of pions and nucleons at finite temperature in the framework of the linear sigma model, and to lowest order in the virial expansion. Results indicate a substantial growth of both widths even at moderately low temperatures.

The temperature behaviour of hadron propagators has been receiving considerable attention [1–5] in connection with the generally accepted possibility of a deconfinement phase transition from hadronic matter to a quark–gluon plasma. Some time ago [6] a proposal was made to consider the hadronic width (damping rate) as a phenomenological order parameter for this phase transition. The idea is that as the critical temperature is approached, hadronic spectral functions should become smooth and describable in terms of just the quark and gluon degrees of freedom. This disappearance of all peaks from the spectrum is achieved by hadronic widths increasing monotonically with temperature. This conjecture received independent confirmation from results of explicit calculations of the pion, nucleon, and rho-meson widths, performed in various theoretical frameworks [2,4,5]. At the same time, these results indicate that hadron masses are fairly independent of temperature [1–5].

Here we study the temperature behaviour of the pion and nucleon widths in the framework of the linear sigma model, and to leading order in the virial expansion. Hadronic mass and width are to be understood, respectively, as the real and imaginary parts of the propagator. The sigma model is relevant, to the extent that it has many of the properties one would expect QCD to exhibit at low energies. At low to moderate temperatures, the virial expansion to leading order is expected to be a reasonable approximation. In this case one has the relation

$$M(\mathbf{p}, T) - \frac{1}{2}i\Gamma(\mathbf{p}, T) = \omega_p - \frac{1}{2\omega_p} \int \frac{d^3q}{(2\pi)^3} \frac{n_B(\omega_q)}{2\omega_q} T(s, 0), \quad (1)$$

where  $n_B$  is the Bose–Einstein statistical factor associated to the one-loop correction due to thermal pions,  $\omega_p = \sqrt{(\mathbf{p}^2 + M^2)}$ , and  $T(s, 0)$  denotes the zero temperature pion–pion or pion–nucleon scattering amplitude, with  $s$  being the square of the center of mass energy. This relation is shown diagrammatically in fig. 1. On account of its heavy mass, sigma-meson loop contributions are strongly Boltzmann suppressed and will then be neglected in the sequel.

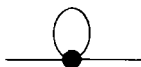


Fig. 1. One-loop thermal pion correction to the  $\pi\pi$  or  $\pi N$  scattering amplitude  $T(s, 0)$  (denoted by the blob).

As it follows from (1), the pion and nucleon widths involve the absorptive parts of the  $\pi$ - $\pi$  and  $\pi$ - $N$  scattering amplitudes at  $T=0$ , which we proceed to calculate starting from the linear sigma model Lagrangian

$$\mathcal{L} = -\frac{\lambda}{3!} v \Phi (\Phi^2 + \pi^2) - g \bar{\psi} (\Phi + i \boldsymbol{\tau} \cdot \boldsymbol{\pi} \gamma_5) \psi - \frac{\lambda}{4!} (\Phi^2 + \pi^2)^2, \quad (2)$$

where  $v = f_\pi \simeq 93$  MeV,  $g = M_N/v$ , and  $\lambda = 3(M_\sigma^2 - \mu_\pi^2)/v^2$ . The relevant diagrams contributing to the imaginary parts of  $T_{\pi\pi}(s, 0)$  and  $T_{\pi N}(s, 0)$  are shown in figs. 2 and 3, respectively, where solid lines represent the pion, dashed lines the sigma-meson, and double solid lines the nucleon. The results of our calculation of the diagrams in fig. 2 are as follows:

$$\text{Im } T_{\pi\pi}^{(a)}(s, 0) = \frac{1}{16\pi} \left(\frac{\lambda}{3}\right)^2 \sqrt{1 - 4 \frac{\mu_\pi^2}{s}} (7\delta_{\alpha\beta}\delta_{\alpha'\beta'} + 2\delta_{\alpha\alpha'}\delta_{\beta\beta'} + 2\delta_{\alpha'\beta'}\delta_{\beta\alpha}) \Theta(s - 4\mu_\pi^2), \quad (3)$$

$$\text{Im } T_{\pi\pi}^{(b)}(s, 0) = \frac{1}{16\pi} \left(\frac{\lambda}{3}\right)^2 \sqrt{1 - 4 \frac{M_\sigma^2}{s}} \delta_{\alpha'\beta'} \delta_{\alpha\beta} \Theta(s - 4M_\sigma^2), \quad (4)$$

$$\text{Im } T_{\pi\pi}^{(c)}(s, 0) = \left(\frac{\lambda v}{3}\right)^2 \frac{\gamma}{(s - M_\sigma^2)^2 + \gamma^2} \delta_{\alpha\beta} \delta_{\alpha'\beta'} \Theta(s - 4\mu_\pi^2), \quad (5)$$

$$\text{Im } T_{\pi\pi}^{(d)}(s, 0) = \frac{1}{8\pi} \left(\frac{\lambda v}{3}\right)^4 \sqrt{1 - 4 \frac{\mu_\pi^2}{s}} \frac{1}{M_\sigma^2(s - 4\mu_\pi^2 + M_\sigma^2)} \delta_{\alpha\alpha'} \delta_{\beta\beta'} \Theta(s - 4\mu_\pi^2), \quad (6)$$

$$\text{Im } T_{\pi\pi}^{(e)}(s, 0) = \frac{1}{16\pi} \left(\frac{\lambda v}{3}\right)^4 \frac{1}{|\mathbf{P}| \sqrt{s}} \left( \frac{1}{x_1^2 + \mu_\pi^2} - \frac{1}{x_2^2 + \mu_\pi^2} \right) \delta_{\alpha\beta} \delta_{\alpha'\beta'} \Theta(|\mathbf{P}|^2 - (M_\sigma^2 - \mu_\pi^2)), \quad (7)$$

where in eq. (5)

$$\gamma = \frac{3}{16\pi} \left(\frac{\lambda v}{3}\right)^2 \sqrt{1 - 4 \frac{\mu_\pi^2}{s}}, \quad (8)$$

and in eq. (7):  $|\mathbf{P}| = \frac{1}{2} \sqrt{s - 4\mu_\pi^2}$ , and

$$x_{1,2} = |\mathbf{P}| \mp \sqrt{|\mathbf{P}|^2 - (M_\sigma^2 - \mu_\pi^2)}. \quad (9)$$

For the diagram shown in fig. 2c, the propagator of the sigma meson has been considered as an effective propagator dressed by the sum of a chain of pion bubbles, consistent with the one-loop order we are dealing with. This

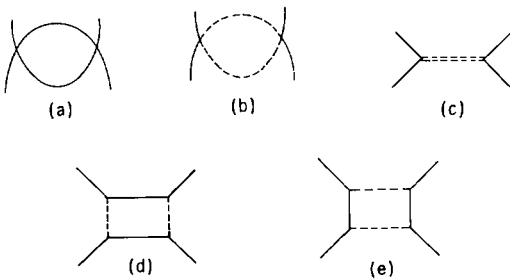


Fig. 2. Contributions to  $T_{\pi\pi}(s, 0)$  from (a): internal pion loop, (b): internal sigma-meson loop, (c): dressed sigma-meson propagator, (d), (e): box loops. Solid and dashed lines represent pions and sigma mesons, respectively. The double dashed line stands for the dressed sigma-meson propagator.

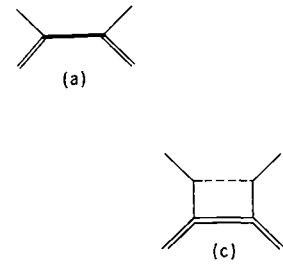


Fig. 3. Contribution to  $T_{\pi N}(s, 0)$  from (a): dressed nucleon propagator, (b), (c): box loops. Solid and dashed lines represent pions and sigma mesons, respectively. The double solid line indicates nucleons, and the bold line stands for the dressed nucleon propagator.

has been indicated in fig. 2c by means of a double dashed line for the sigma propagator, which then develops a real and an imaginary part of its own.

Proceeding to the absorptive part of the pion-nucleon scattering amplitude, the results we find for the diagrams shown in fig. 3 are

$$\begin{aligned} \text{Im } T_{\pi N}^{(a)}(s, 0) &= \frac{2g^2}{D} \{E_N[a(2ab - 2M_N\sqrt{s}) - b(s + M_N^2 + a^2 + b^2)] + M_N[a(s + M_N^2 + a^2 + b^2) - b(2ab - 2M_N\sqrt{s})]\} \tau_\alpha \tau_\beta \\ &\times \Theta(s - (M_N + \mu_\pi)^2), \end{aligned} \quad (10)$$

where

$$a = \frac{3g^2}{4\pi} \frac{|Q|}{\sqrt{s}} M_N, \quad b = -\frac{3g^2}{4\pi} \frac{|Q|}{\sqrt{s}} E_N, \quad (11)$$

$$|Q| = \frac{1}{2\sqrt{s}} \{[s - (M_N + \mu_\pi)^2][s - (M_N - \mu_\pi)^2]\}^{1/2}, \quad E_N = \frac{s + M_N^2 - \mu_\pi^2}{2\sqrt{s}}, \quad (12,13)$$

$$D = (s + M_N^2 + a^2 + b^2)^2 - 4(a^2b^2 + sM_N^2 - 2abM_N\sqrt{s}), \quad (14)$$

$$\begin{aligned} \text{Im } T_{\pi N}^{(b)}(s, 0) &= \frac{g^2}{4\pi} \left(\frac{\lambda v}{3}\right)^2 \frac{1}{|Q|\sqrt{s}} \left[ M_N^2 \left( \frac{1}{M_\sigma^2} - \frac{1}{4|Q|^2 + M_\sigma^2} \right) - \frac{|Q|^2}{4|Q|^2 + M_\sigma^2} + \frac{1}{4} \ln \left( \frac{4|Q|^2 + M_\sigma^2}{M_\sigma^2} \right) \right] \delta_{i\alpha\beta} \\ &\times \Theta(s - (M_N + \mu_\pi)^2), \end{aligned} \quad (15)$$

$$\begin{aligned} \text{Im } T_{\pi N}^{(c)}(s, 0) &= \frac{g^2}{16\pi} \left(\frac{\lambda v}{3}\right)^2 \frac{1}{|Q|\sqrt{s}} \left[ \ln \left( \frac{y_1^2 + \rho^2}{y_2^2 + \rho^2} \right) + \left( \frac{1}{y_1^2 + \rho^2} - \frac{1}{y_2^2 + \rho^2} \right) \left( (M_\sigma^2 - \mu_\pi^2) \frac{E_N}{\sqrt{s}} - |z| + \rho^2 \right) \right] \tau_\alpha \tau_\beta \\ &\times \Theta(|Q|^2 - |z|), \end{aligned} \quad (16)$$

with

$$\rho^2 = \mu_\pi^2 - \frac{(M_\sigma^2 - \mu_\pi^2)^2}{4s}, \quad y_{1,2} = |Q| \mp \sqrt{|Q|^2 - |z|}, \quad (17)$$

and  $x = (M_\sigma^2 - \mu_\pi^2)/2\sqrt{s}$ ,  $z = x^2 + 2E_N x - (M_\sigma^2 - \mu_\pi^2)$ , and  $E_N = \sqrt{|Q|^2 + \mu_\pi^2}$ . In the diagram of fig. 3a the nucleon propagator is shown as a bold line, corresponding to an effective propagator dressed by a chain of pion loops. In the expressions given above for the absorptive parts of the  $\pi$ - $\pi$  and  $\pi$ - $N$  scattering amplitudes, the sigma-meson mass is a free parameter which we vary in the range  $M_\sigma = 400$ – $800$  MeV. All masses are assumed temperature independent, in line with results from various theoretical approaches [1–5].

After substituting these imaginary parts in eq. (1) we obtain the pion and nucleon widths shown in figs. 4 and 5, respectively. Since these widths strictly vanish at  $T=0$ , the effect of temperature is rather dramatic, even at moderate values of  $T$  where we expect the leading order in the virial expansion to be a reasonable approximation. These hadronic thermal widths should be interpreted as the damping coefficients of wave packets propagating through a dispersive medium (heat bath). Their growth with increasing temperature implies that, with hadrons corresponding to excitations in this medium, these excitations become less and less important. Combined with the notion of quark-hadron duality, this may be interpreted as the melting of hadrons into their quark constituents, thus signalling a deconfinement phase transition. Aside from its intrinsic interest, knowledge of the temperature dependence of hadronic propagators, particularly pion and rho-meson propagators, is important in connection with heavy ion collisions at very high energies. In fact, some time ago [7] it was shown that a rho-meson width which increases with temperature has an important impact on the dilepton production rate in these nuclear collisions.

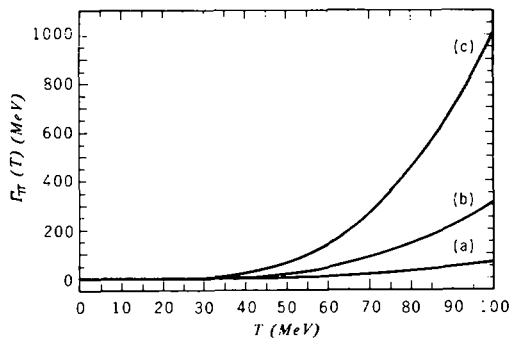


Fig. 4. Temperature behaviour of the pion width for  $M_\sigma=400$  MeV (a), 600 MeV (b), and 800 MeV (c).

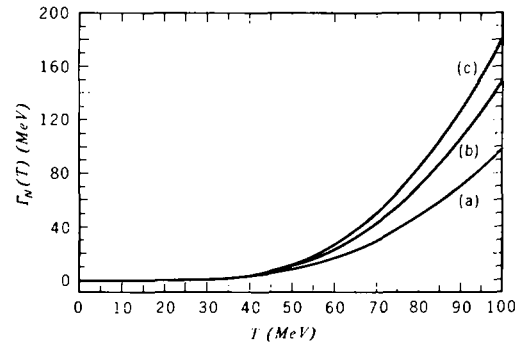


Fig. 5. Temperature behaviour of the nucleon width for  $M_\sigma=400$  MeV (a), 600 MeV (b), and 800 MeV (c).

The work of C.A.D. has been supported in part by the Foundation for Research Development (South Africa), that of M.L. by FONDECYT 0751/92C (Chile), and that of J.C.R. by FONDECYT 0047/92. This work has been carried out in the framework of the FRD-CONICYT Scientific Exchange Program.

## References

- [1] A. Larsen, *Z. Phys. C* 33 (1986) 291;  
C. Contreras and M. Loewe, *Intern. J. Mod. Phys. A* 5 (1990) 2297.
- [2] J. Goity and H. Leutwyler, *Phys. Lett. B* 228 (1989) 517;  
H. Leutwyler and A.V. Smilga, *Nucl. Phys. B* 342 (1990) 302.
- [3] A. Barducci, R. Casalbuoni, S. DeCurtis, R. Gatto and G. Pettini, *Phys. Rev. D* 46 (1992) 2203.
- [4] A. Schenk, *Nucl. Phys. B* 363 (1991) 97.
- [5] C.A. Dominguez and M. Loewe, *Z. Phys. C* 58 (1993) 273;  
C.A. Dominguez, M. Loewe and J.C. Rojas, *Z. Phys. C* 59 (1993) 63.
- [6] C.A. Dominguez and M. Loewe, *Phys. Lett. B* 233 (1989) 201; *Nucl. Phys. B (Proc. Suppl.)* 16 (1990) 403.
- [7] C.A. Dominguez and M. Loewe, *Z. Phys. C* 49 (1991) 423.